Supplementary Information: Phase Diagram of Water Confined by Graphene

Zhenghan Gao,[†] Nicolas Giovambattista,[*,‡,¶] and Ozgur Sahin[*,†,§]

†*Department of Physics, Columbia University, New York City, NY 10027 USA*

‡*Departments of Physics, Brooklyn College of the City University of New York, Brooklyn, NY 11210 USA*

¶*PhD Programs in Physics and Chemistry, The Graduate Center of the City University of New York, New York City, NY 10027 USA*

§*Department of Biological Sciences, Columbia University, New York City, NY 10027 USA*

E-mail: NGiovambattista@brooklyn.cuny.edu; os2246@columbia.edu

S1. A brief thermodynamic description of a liquid confined in slab geometry

Here, we provide a brief thermodynamic description of a liquid confined in slab geometry. In particular, we show that for such a system to be thermodynamically stable, it must be that:

$$\left(\frac{\partial P_{\perp}}{\partial D}\right)_{T,N,A} < 0 \tag{1}$$

The first law of thermodynamics states that

$$\mathrm{d}U = T\mathrm{d}S - \mathrm{d}W + \mu\mathrm{d}N \tag{2}$$

where S is the entropy, μ is the chemical potential, and $\mathrm{d}W$ represents the mechanical work done on the system. For a liquid confined in slab geometry (see, e.g. Refs.[1–3]), isotropic along the direction parallel to the graphene sheets, the mechanical work can be expressed as

$$\mathrm{d}W = P_{\parallel} D\mathrm{d}A + P_{\perp} A\mathrm{d}D \tag{3}$$

where $P_{\parallel}$ and $P_{\perp}$ are, respectively, the pressure along the direction parallel and perpendicular to the graphene sheets. From Eqs. 2 and 3, it follows that the Helmholtz free energy F obeys

$$\mathrm{d}F = \mathrm{d}(U - TS) = -S\mathrm{d}T - P_{\parallel} D\ \mathrm{d}A - P_{\perp} A\ \mathrm{d}D + \mu\mathrm{d}N \tag{4}$$

If the walls surface area is constant, as it is the case in our MD simulations, then

$$\mathrm{d}F = -S\mathrm{d}T - P_{\perp}\ \mathrm{d}V + \mu\mathrm{d}N \tag{5}$$

Eq. 5 is analogous to the expression of dF for the case of a bulk liquid where $P_{\perp}$ plays the role of the bulk liquid pressure P. It follows that the condition of stability for a bulk liquid, $\left(\frac{\partial^2 F}{\partial^2 V}\right)_{T,N} > 0$, holds for our confined liquid ($A = constant$). Therefore, the condition of stability for a confined liquid in slab geometry, with constant wall surface area, is

$$\left(\frac{\partial P_{\perp}}{\partial D}\right)_{T,N,A} < 0 \tag{6}$$

S2. Continuous bilayer ice-liquid transformation

As shown in Fig.5b of the main manuscript, the transformation between the bilayer ice and the liquid is a first-order phase transition for $\sigma > 25.60$ nm^{-2} (star in Fig.5b). An example of this first-order phase transition is shown in Fig.4 of the main manuscript for $\sigma = 27.73$ nm^{-2}. Here, we describe briefly the case of a continuous bilayer ice-liquid transformation for the case $\sigma = 25.60$ nm^{-2}.

Fig.S1a shows $P_{\perp}(D)$ for $\sigma = 25.60$ nm^{-2}. A comparison with Fig.4a shows that at $\sigma = 25.60$ nm^{-2} there is only one instability region at $D = 1.21$ nm due to the liquid-vapor phase transition, with no signature of a bilayer ice-liquid first-order phase transition. Yet, we observe that at very small D, the system crystallizes into the same bilayer ice reported at $\sigma = 27.73$ nm^{-2}.

Evidences of the bilayer ice-liquid transformation occurs is provided in Figs. S1(b)-(d), where we include the radial distribution function, MSD, and density profile of water at selected values of D. Specifically, Figs. S1b indicates that water molecules arrange into two monolayers at all graphene sheet separations. Figs. S1(c) and (d) indicate that as $D \to 0.77$ nm, the MSD decreases rapidly and becomes almost constant for $D \approx 0.77$ nm while, simultaneously, the RDF of water exhibits more pronounced extrema. In other words, for $D \approx 0.77$ nm, liquid water becomes ice. We note that the location of maxima and minima in the RDF of Fig.S1(d) for $D = 0.77$ nm and in Fig.4d of the main manuscript are identical, indicating that the same bilayer ice forms at both surface densities.

S3. Effects of Water-graphene interactions on the Phase Behavior of Confined Water

The contact angle of water in contact with graphene is approximately $\theta_c = 96^{\circ}$ in theory,[4] but experimental results vary, finding $90 \leq \theta_c \leq 108^{\circ}$.[5–7] Our results are based on water

O-graphene C interactions with a Lennard Jones ϵ_{CO} parameter of $\epsilon_{CO} = 0.15104$ kJ/mol which was chosen in order to reproduce a water contact angle of $\theta_c = 108°$. A natural question is whether the phase behavior of water confined between graphene sheets reported in the main manuscript is sensitive to the specific water O-graphene C interactions chosen. In order to address this question, we perform MD simulations for the same system shown in Fig.1a of the main manuscript but where $\epsilon_{CO} = 0.26860$ kJ/mol. For this value of ϵ_{CO}, we find that $\theta_c = 90°$.

In Fig.S2, we show the behavior of $P_\perp(D)$ for selected values of sigma for $\epsilon_{CO} = 0.15104$ kJ/mol ($\theta_c = 108°$, solid lines) and $\epsilon_{CO} = 0.26860$ kJ/mol ($\theta_c = 90°$, dashed lines). It follows from Fig.S2 that the phase behavior of water confined by graphene sheets is indeed robust relative to variations in water-graphene interactions with only minor changes for $90° \leq \theta_c \leq 108°$.

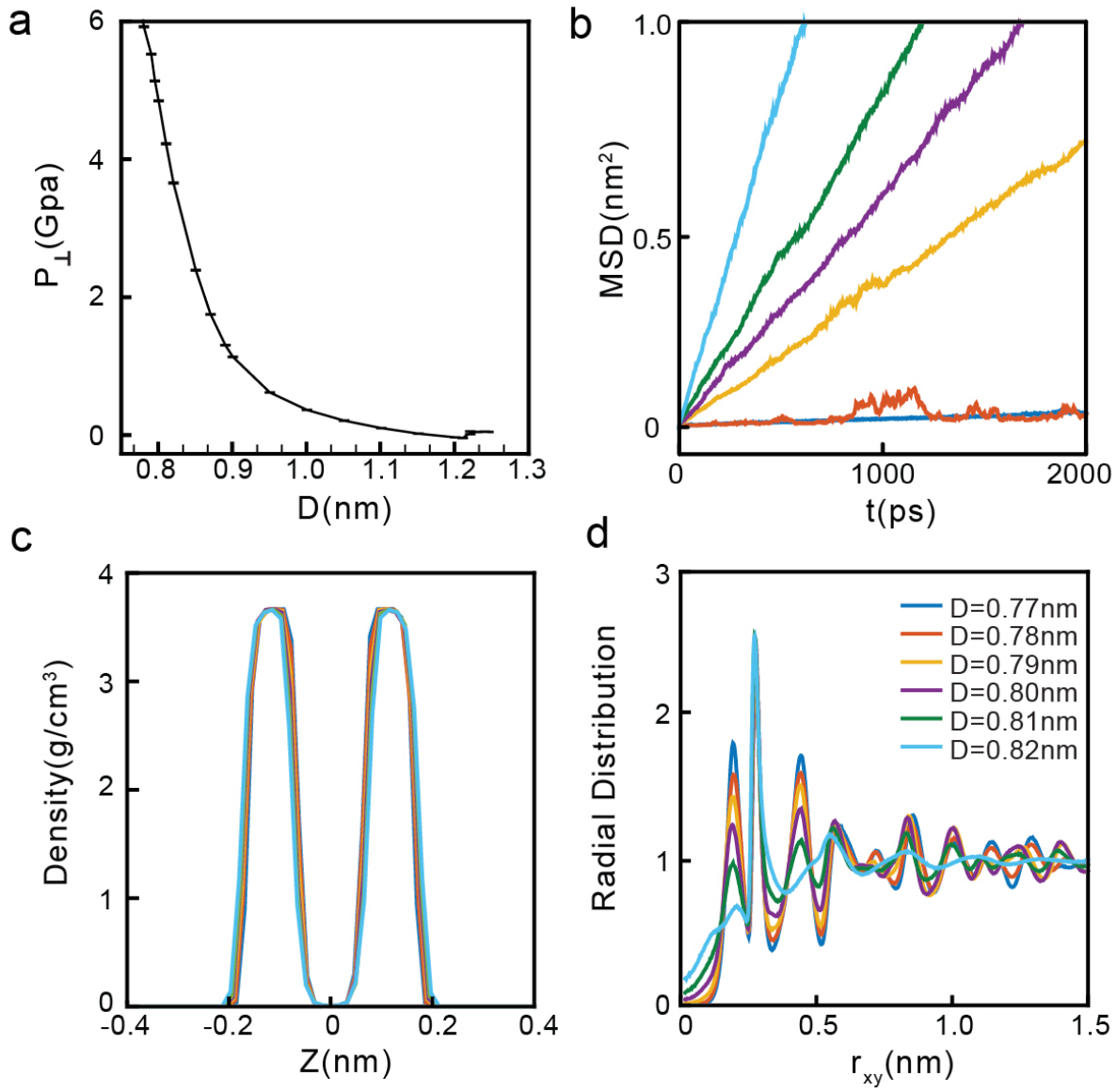

Fig.S1: *Continuous* bilayer ice-liquid transition at $\sigma = 25.60$ nm^{-2}. (a) $P_\perp - D$ curve. (b) Mean square displacement. (c) Transverse density profile along z direction. (d) Lateral Oxygen-Oxygen radial distribution.

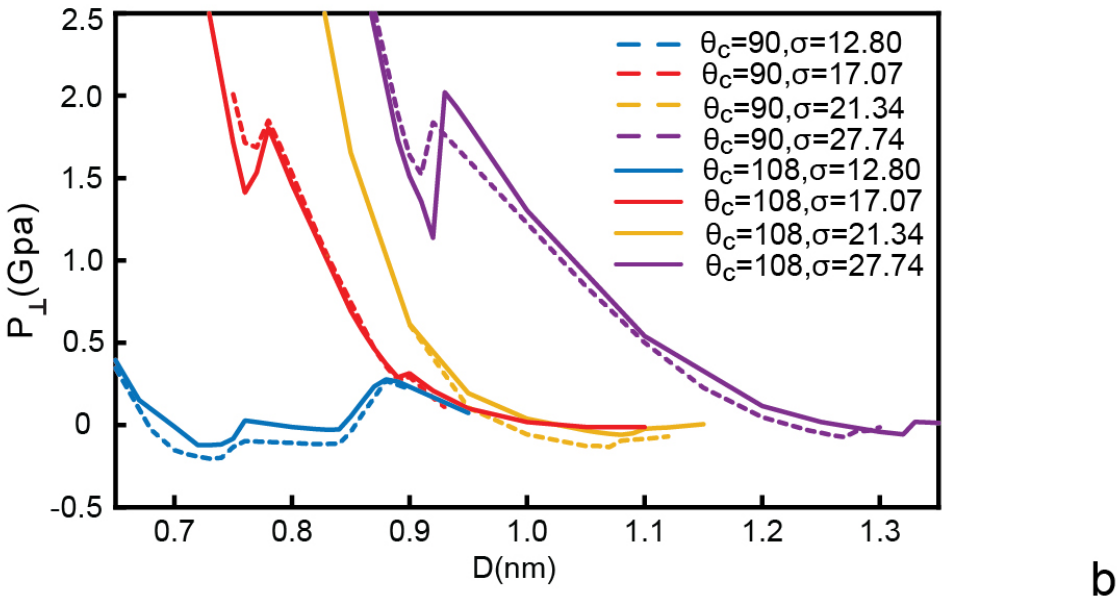

Fig.S2: Pressure perpendicular to the graphene sheets for selected surface densities σ. Solid lines are taken from Fig.1a of the main manuscript and correspond to water O-graphene C interactions with Lennard-Jones parameter $\epsilon_{CO} = 0.15104$ kJ/mol ($\theta_c = 108°$). Dased lines correspond to $\epsilon_{CO} = 0.26860$ kJ/mol ($\theta_c = 90°$). In both cases, we find basically the same phase behavior of water indicating that our results are robust relative to variations in ϵ_{CO} (θ_c).

References

1. Klapp, S.; Schoen, M. *Reviews In Computational Chemistry*; 2007; Vol. 24.

2. Truskett, T. M.; Debenedetti, P. G.; Torquato, S. Thermodynamic implications of confinement for a waterlike fluid. *The Journal of Chemical Physics* **2001**, *114*, 2401–2418.

3. Giovambattista, N.; Rossky, P. J.; Debenedetti, P. G. Phase transitions induced by nanoconfinement in liquid water. *Physical review letters* **2009**, *102*, 050603.

4. Shih, C.-J.; Wang, Q. H.; Lin, S.; Park, K.-C.; Jin, Z.; Strano, M. S.; Blankschtein, D. Breakdown in the wetting transparency of graphene. *Physical review letters* **2012**, *109*, 176101.

5. Shin, Y. J.; Wang, Y.; Huang, H.; Kalon, G.; Wee, A. T. S.; Shen, Z.; Bhatia, C. S.; Yang, H. Surface-energy engineering of graphene. *Langmuir* **2010**, *26*, 3798–3802.

6. Wang, S.; Zhang, Y.; Abidi, N.; Cabrales, L. Wettability and surface free energy of graphene films. *Langmuir* **2009**, *25*, 11078–11081.

7. Rafiee, J.; Mi, X.; Gullapalli, H.; Thomas, A. V.; Yavari, F.; Shi, Y.; Ajayan, P. M.; Koratkar, N. A. Wetting transparency of graphene. *Nature materials* **2012**, *11*, 217–222.